

## AN ABSTRACT OF THE THESIS OF

Dong-Wook Kim for the degree of Master of Science in Forest Engineering  
presented on June 6, 2012

Title: Modeling Air-Drying of Douglas-fir and Hybrid Poplar Biomass in Oregon

Abstract approved:

---

Glen E. Murphy

Both transportation costs and market values of woody biomass are strongly linked to the amount of moisture in the woody biomass. Therefore, managing moisture in the woody biomass well can lead to significant advantages in the woody biomass energy business. In this study, two prediction models were developed to estimate moisture content for Douglas-fir (*Pseudotsuga menziesii* (Mirb.) Franco) and hybrid poplar (*Populus* spp.) woody biomass. Experimental data for the Douglas-fir model were collected over four different seasons at two different in-forest study sites in Oregon (Corvallis and Butte Falls) between December 2010 and December 2011. Three woody biomass bundles consisting of 3-meter length logs (30 to 385 mm diameter) were built each season at each study site; a total of 24 Douglas-fir bundles (1,316 to 3,621 kg weight) were built

over the period. Experimental data for the hybrid poplar model were collected in two drying trials at two off-forest study sites in Oregon (Clatskanie and Boardman) between April 2011 and January 2012. Two types of woody bundles consisting of 3-meter length logs were built each trial: small (28 to 128 mm diameter, 2,268 to 5,389 kg weight) and large (75 to 230 mm diameter, 3,901 to 7,013 kg weight). A total of eight hybrid poplar bundles were built over the period. These data were used to develop linear mixed effects multiple regression models for predicting the moisture content of Douglas-fir and hybrid poplar biomass, respectively. The major factors considered in this study for predicting woody biomass moisture content change were cumulative precipitation, evapotranspiration ( $ET_0$ ), and biomass piece size. The Food and Agriculture Organization (FAO) Penman-Monteith method, which requires temperature, solar radiation, wind, and relative humidity data, was used to calculate  $ET_0$ . The developed models can be easily applied to any location where historic weather data are available to calculate estimated air-drying times for Douglas-fir and hybrid poplar biomass at any time of the year. Oregon has been split into nine climate zones. Use of the model was demonstrated for four climate zones, two in which air-drying data were collected, and two in which it was not collected. Considerable differences in predicted drying times were observed between the four climate zones.

©Copyright by Dong-Wook Kim

June 6, 2012

All Rights Reserved

Modeling Air-Drying of Douglas-fir and Hybrid Poplar Biomass in Oregon

by

Dong-Wook Kim

A THESIS

submitted to

Oregon State University

in partial fulfillment of

the requirements for the

degree of

Master of Science

Presented June 6, 2012

Commencement June 2013

Master of Science thesis of Dong-Wook Kim presented on June 6, 2012.

APPROVED:

---

Major Professor, representing Forest Engineering

---

Head of the Department of Forest Engineering, Resources and Management

---

Dean of the Graduate School

I understand that my thesis will become part of the permanent collection of Oregon State University libraries. My signature below authorizes release of my thesis to any reader upon request.

---

Dong-Wook Kim, Author

## ACKNOWLEDGEMENTS

Funding for this project has been provided by the USDA Special Grants program for Wood Utilization Research.

I would like to thank; Jeff Wimer and Oregon State University (OSU) Student Logging Crew (Corvallis); Ron and Troy of Ron Hailicka Equipment Inc. (Butte Falls, Oregon); Bruce Summers and Gary Gressett in GreenWood Resources (Boardman and Clatskanie, Oregon) for their great support for these drying trials. Support came in three forms (1) providing woody biomass, (2) providing equipment to build bundles and weigh them regularly, and (3) providing personnel to help build and weigh bundles. Without their support this project could not have been undertaken.

Especially, I would like to express my unreserved thanks to Dr. Glen Murphy, my major professor, who always encouraged and advised me. Without his support my thesis study would never have been completed.

I would like to thank my committee members, Dr. Michael Wing, Dr. John Bailey, and Dr. Sarah Emerson for their critical reflections on this study. In particular, I want to thank Dr. Bailey for his critical review comments and advice for my thesis.

I would like to express my deepest gratitude to Dr. John Sessions and Dr. Loren Kellogg for their valuable advice and incredible support during my study period at OSU.

I also want to thank my friends, Dr. Sang-Kyun Han, Yo-Han Lee, Dr. Jung-Il Seo, Fernando Becerra, Storm Beck, Kelsey Lee, Jennifer Barnett, and Rene Zamora for their wonderful help throughout my MS study.

In addition, I would like to thank my father Sung-Nam Kim, my mother Jung-Hee Pee, my father-in-law Ki-Seong Kim, and my mother-in-law In-Hae Kim for their unconditional support and powerful encouragement.

Finally, I would like to mention the source of my motivation, my lovely wife Hae-Min Kim and awesome sons, Min-Sub & Min-Sung.

## CONTRIBUTION OF AUTHORS

I would like thank Dr. Glen Murphy for his considerable contribution to this document. His contributions included assistance with study design, data collection, and final document revision.



## TABLE OF CONTENTS

	<u>Page</u>
CHAPTER 1: INTRODUCTION.....	1
1.1    Background .....	1
1.2    Research objectives.....	4
CHAPTER 2: LITERATURE REVIEW.....	6
2.1    Previous drying studies .....	6
2.2    The FAO Penman-Monteith method .....	9
CHAPTER 3: STUDY METHODS.....	11
3.1    Data collection.....	11
3.1.1    Drying trials data .....	11
3.1.1.1    Study sites description.....	11
3.1.1.2    Biomass bundles .....	12
3.1.1.3    Woody disks.....	14
3.1.2    Weather data.....	15
3.2    Modeling .....	16
3.2.1    Data preparation .....	16
3.2.2    Drying models .....	17

## TABLE OF CONTENTS (Continued)

	<u>Page</u>
CHAPTER 4: RESULTS AND DISCUSSION .....	20
4.1    Actual drying times.....	20
4.1.1    Douglas-fir .....	20
4.1.2    Hybrid poplar .....	22
4.2    Prediction models .....	24
4.3    Validation of prediction models .....	26
4.4    Predicted air-drying times .....	30
4.4.1    Prediction of air-drying days for Douglas-fir biomass .....	31
4.4.2    Prediction of air-drying days for hybrid poplar biomass .....	32
4.4.2.1    Small hybrid poplar.....	32
4.4.2.2    Large hybrid poplar.....	34
4.4.2.3    Comparison of drying rates for large and small poplar.....	35
CHAPTER 5: CONCLUSIONS .....	36
5.1    General conclusions and limitations .....	36
5.2    Management implications .....	38
BIBLIOGRAPHY .....	40

## TABLE OF CONTENTS (Continued)

	<u>Page</u>
APPENDIX A: Figures and tables relating to the drying trials.....	45
APPENDIX B: Formulas to calculate the reference evapotranspiration .....	51

## LIST OF FIGURES

<u>Figure</u>	<u>Page</u>
3.1 Map of study sites: representing locations of four study sites in Oregon which are Clatskanie, Boardman, Corvallis, and Butte Falls. ....	12
4.1 Drying curves of Douglas-fir biomass drying trials at Corvallis, OR (A) and at Butte Falls, OR (B). In the legends below each figure the first letter (or two) relates to the season in which drying began (W = Winter, S = Spring, Su = Summer, F = Fall), the middle letter relates to the study location (C = Corvallis, B = Butte Falls), the last letter relates to the canopy cover type (O = Open, I = Intermediate, C = Closed).....	21
4.2 Drying curves of both small and large hybrid poplar biomass drying trials at Clatskanie (A) and at Boardman, OR (B). In the legends below each figure 1 <sup>st</sup> = the first trial, 2 <sup>nd</sup> = the second trial, Large = large biomass bundles and Small = small biomass bundles.....	23
4.3 Relationships between actual and predicted moisture content for both Douglas-fir biomass (a) and hybrid poplar biomass (b).....	27
4.4 Actual and predicted drying curves for Douglas-fir biomass for two bundles chosen to represent the best (a) and worst (b) fits .....	28
4.5 Actual and predicted drying curves for hybrid poplar biomass for two bundles chosen to represent the best (a) and worst (b) fits .....	29
A.1 The map of Oregon Climate Zones with the general locations of sites used for predicting air-drying times. ( <a href="http://oregon.gov/ODA/NRD/weather.shtml#Weather_forecasts">http://oregon.gov/ODA/NRD/weather.shtml#Weather_forecasts</a> ) .....	45

## LIST OF FIGURES (Continued)

<u>Figure</u>	<u>Page</u>
A.2 Douglas-fir bundle construction using a large hydraulic loader (above) and air-drying Douglas-fir bundles under the intermediate canopy cover (bottom) ....	49
A.3 Cross section of the large hybrid poplar bundle (above) and weighing a small hybrid poplar bundle using a crane scale and large hydraulic loader (bottom)	50

## LIST OF TABLES

<u>Table</u>	<u>Page</u>
4.1 Total precipitation and reference evapotranspiration at four locations in Oregon for the period 1 January 2010 to 31 December 2011 .....	30
4.2 Predicted number of days required to dry Douglas-fir biomass to 30% moisture content at four Oregon climate zones depending on different start months. ....	31
4.3 Predicted number of days required to dry small hybrid poplar biomass to 30% moisture content at four Oregon climate zones depending on different start months. ....	33
4.4 Predicted number of days required to dry large hybrid poplar biomass to 30% moisture content at four Oregon climate zones depending on different start months. ....	34
4.5 Ratio of predicted number of days required to dry large hybrid poplar biomass, compared with small hybrid poplar biomass, to 30% moisture content at four Oregon climate zones depending on different start months. ....	35
A.1 Information relating to Douglas-fir bundles at Corvallis .....	46
A.2 Information relating to Douglas-fir bundles at Butte Falls.....	47
A.3 Information relating to hybrid poplar bundles at Clatskanie .....	48
A.4 Information relating to hybrid poplar bundles at Boardman .....	48

## DEDICATION

This thesis is dedicated to my father, Sung-Nam Kim.

# **Modeling Air-Drying of Douglas-fir and Hybrid Poplar Biomass in Oregon**

## **CHAPTER 1**

### **INTRODUCTION**

#### **1.1 Background**

Biomass energy is any non-fossil energy derived from biomass. Biomass is any organic matter that is available on a renewable or recurring basis. Biomass has become a significant fuel source, particularly in the U.S. due to “costly and dangerous dependence on fossil fuel” (Payne et al. 2009). A 2005 USDA study identified biomass as an alternative to fossil fuels with the potential to replace up to 30% of petroleum usage by 2030 (Perlack et al. 2005). Moreover, biomass is now the single largest source of renewable energy, recently surpassing other renewable energy sources: hydropower, wind, geothermal, and solar (Perlack et al. 2005). Dependence on biomass has been increasing gradually and is over 4% of the U.S. total energy consumption (Energy Information Administration 2010). In addition, wood is an important alternative energy source due to its high contribution to biomass energy. Wood accounts for about 50% of total biomass energy of the U.S. in 2010 (Energy Information Administration 2010).

Woody biomass is one source of biomass energy. There are three main sources of woody biomass: wood residue, wood waste, and woody plants (Robert



2007). Wood residue includes small branches, tree thinning materials, tree tops, and other wood from harvested trees. Wood waste includes bark, sawdust, shaving, and off-cuts of processed wood in dimensional lumber, post and pole operations, and plywoods. Woody plants are crop plantations such as tree farms with short rotations. Over a billion dry tons per year would be available from forest and agricultural sources and from recycled wood from urban waste. It has been estimated that the total amount of forest biomass that can be produced annually in the U.S is 368 million dry tons (Perlack et al. 2005).

Compared to fossil fuel, there are many environmental advantages in using woody biomass for energy. Wood is a renewable resource as long as the forest is under sustainable harvesting systems. Also, low levels of carbon dioxide (CO<sub>2</sub>), heavy metals, and sulfur are emitted by burning wood fuel (Bergman and Zerbe 2004).

However, there are some challenges that limit woody biomass use as an energy source. The main barriers to woody biomass use are found in the forest biomass feed stock systems: the high cost of harvesting, transportation, and storage (Biomass Research and Development Technical Advisory Committee & Biomass Research and Development Initiative 2007). These barriers mean that woody biomass is not economically attractive relative to its market values (Rummer 2008). Even though the U.S. government provides substantial subsidies to expanding the role of biomass as an energy source, compared to fossil fuels, woody biomass is still not an economically attractive energy source due to its high production costs (Perlack et al. 2005; Energy Information Administration 2010).

Managing moisture is a key to improving the economic feasibility in woody biomass use (Jirjis 1995). Transportation costs and market values of woody biomass are strongly linked to the amount of moisture in the woody biomass (Kofman and Kent 2007). The cost of transportation is the largest single component of total production costs in the biomass feedstock supply chains; about 47 to 50% of total production costs were reported as the transportation costs (McDonald et al. 2001, Pan et al. 2008). Ronnqvist et al. (1998) stated that small improvements in transportation efficiency could remarkably reduce total production costs for woody biomass energy. Also, McDonald et al. (1995) comment that optimizing transport of energy wood generally requires carrying the greatest possible amount of material per load due to its low market value. Green wood contains approximately 50 percent water by weight. Thus, reducing the amount of water in woody biomass can lead to carrying more wood and less water per load. Also, reducing water in wood could allow reductions in the transportation costs due to lower energy consumption for delivering the same amount of woody biomass. T. Liang et al. (1996) showed that the effect of moisture is more critical for energy use efficiency in the high moisture range (such as over 50%). They reported that woody biomass energy efficiency improves 1% for each 1% drop of moisture over 50% and 0.5% for each 1% drop of moisture below 40%. They also reported that the energy conversion facility size increases 2% for each 1% increase of moisture over 50% and 1% for each 1% increase in moisture in the woody biomass between 25 and 35%. Therefore, good management of woody biomass moisture can lead to significant advantages in woody biomass use as an energy source.

There are a number of critical factors that should be considered for managing moisture in woody biomass feedstock chains: the size and species of tree, the season in which harvesting is carried out, and the material form of the woody biomass. Initial moisture content and the rate of moisture change are affected by tree size, species, and season (Simpson and Wang 2003, Pettersson and Nordfjell 2007). The material form effects rate of moisture change. Johansson et al. (2006) also noted that transportation costs varied depending on the form of the woody biomass, shredded, chipped, or bundled.

## **1.2 Research objectives**

The ultimate objective of this study was to develop new methods based on moisture management that can be used to improve the economic feasibility of woody biomass use for energy. Being able to predict the number of days required to reach a specified moisture content is one of the essential prerequisites for selecting the economically optimal drying method and length of time. This study was focused on investigating the changes in woody biomass moisture content that occur with changing weather conditions.

Specific research objectives were: (1) to measure changes in moisture content for Douglas-fir (*Pseudotsuga menziesii* (Mirb.) Franco) and hybrid poplar (*Populus* spp.) harvested at different locations in Oregon and at different times of the year, (2) to develop climate-based prediction models that can be used to estimate drying times for these species at any time of the year and at any location

where historic weather data are available, and (3) to demonstrate uses of these models for predicting variation in drying times between different climate zones in Oregon.

## **CHAPTER 2**

### **LITERATURE REVIEW**

The purpose of this chapter is: (1) to briefly present what kinds of factors were considered in previous studies related to woody biomass air-drying modeling and (2) to briefly describe the Food and Agriculture Organization (FAO) Penman-Monteith method which was used to calculate reference evapotranspiration ( $ET_0$ ) in this study.

#### **2.1 Previous drying studies**

Over more than half a century studies have been done to understand factors influencing moisture content changes in wood. Many factors have been identified that affected moisture content in wood, including the size, form, and species of the woody biomass, the harvesting seasons and the number of days since drying began, the presence or absence of cover of the biomass, and climate conditions such as temperature, relative humidity, and rainfall. Among the factors, ambient weather conditions were commonly considered as major factors determining moisture content changes.

Stokes et al. (1987) developed moisture content prediction models for groups of softwood and hardwood species and for individual species in the southeastern United States. Their models were non-linear and considered many variables, including number of days since drying began, rainfall, temperature,

bundle weights, and diameter at breast height. They built a total of forty different models to predict a weight reduction factor which was the percent reduction in weight compared to the initial bundle weight. Since they found that average daily temperature alone did not adequately explain the differences in drying rates between the summer and winter season, they suggested using separate equations for different times of the year.

Jirjis (1995) showed that moisture content decreased at a faster rate in covered wood materials in comparison with uncovered wood materials. He also noted that, in comparison to storing wood stored in a chip form, storing wood in an uncomminted form eliminated the risks of self-ignition and allergic reactions and minimized dry matter losses.

Liang et al. (1996) developed a model for predicting the moisture content of bundled *Leucaena* (*Leucaena leucocephala* (Lam.) de Wit) trees in Hawaii. In order to develop a practical model which could be extended spatially to other parts of Hawaii and temporally to different seasons of the year, they developed a prediction model based on environmental conditions. The major environmental factors considered in their model were precipitation and reference evapotranspiration which was computed using Hargreave's model. Their model can be used to predict final moisture content as a function of initial moisture content, number of days since drying began, precipitation and evapotranspiration.

Simpson et al. (1999) described many factors that influence drying rate of green lumber: species, thickness, grain patterns, sapwood and heartwood, piling

methods, height and type of pile foundation, yard surface, and climate. Since specific gravity<sup>1</sup> of wood is different depending on species, each tree species has different drying rates; generally, the lower density species will dry faster than the higher density species (Simpson et al. 1999). The effect of thickness is critical to drying time. A common rule of thumb used by the US forest industry is that drying time increases at the rate of approximately the thickness raised to the 1.5 power (Simpson et al. 1999). Usually sapwood<sup>2</sup> contains much more moisture than heartwood<sup>3</sup> in softwoods; however, sapwood dries faster than heartwood (Simpson et al. 1999). On the other hand, there is not much difference in the amount of moisture between sapwood and heartwood in hardwoods (Simpson et al. 1999). Lumber dries faster in air-drying with spaces between drying materials (Simpson et al. 1999). In addition, Simpson et al. (1999) showed that drying times differed depending on different climate regions in the U.S.

Simpson and Wang (2003) developed two models for estimating air-drying times of small diameter ponderosa pine (*Pinus ponderosa* Douglas ex. C. Lawson) and Douglas-fir logs in the western United States. The logs were debarked and stacked at four different times of the year. The stacks were covered with plywood to protect the logs from rainfall and direct sun exposure. Their two multiple

---

<sup>1</sup> Specific gravity is defined by Simpson et al. (1999) as “the ratio of the oven-dry weight of a piece of wood to the weight of an equal volume of water at 4°C (39°F). Specific gravity of wood is usually based on the green volume.”

<sup>2</sup> Sapwood is the outer layers of the stem in the living tree that contain living cells and is the tree’s pipeline for water (Simpson et al. 1999).

<sup>3</sup> Heartwood is the inner layers of the tree that contain the dead portion of the tree (Simpson et al. 1999).

linear and nonlinear regression models were developed to estimate daily loss of moisture content based on log diameter, starting moisture content, average temperature, and relative humidity. Their study showed that the drying rate changes depending on log diameter size and climate conditions.

Pettersson and Nordfjell (2007) mentioned that biological losses of mass can occur due to blue stain and rot fungus in woody biomass. However, the size of the losses caused by them is insignificant. Thus, the effects of blue stain and rot fungus are not considered in this study.

Based on the previous studies, precipitation (a combination of rainfall and snowfall (Trenberth 1998)) and reference evapotranspiration ( $ET_0$ ) were chosen as the major weather factors to be included in this study. Additional factors included species, log size and canopy cover.

## **2.2 The FAO Penman-Monteith method**

Evapotranspiration is a term describing the sum of soil evaporation and crop transpiration (Labedski et al. 2011). There are three types of evapotranspiration; potential, actual, and reference. The potential evapotranspiration is defined as the amount of evaporation that would occur under unlimited soil water supply and actual meteorological conditions (Thornthwaite 1948). The actual evapotranspiration is defined as the amount of water actually transpired and evaporated under actual meteorological conditions (Thornthwaite



1948). The reference evapotranspiration is the amount of evapotranspiration from a reference surface and is denoted as  $ET_0$  (Allen et al. 1998).

$ET_0$  is an important agrometeorological parameter for climatological and hydrological studies, as well as for irrigation planning and management (Sentelhas et al. 2010). There are several methods to estimate  $ET_0$ ; however, the FAO Penman-Monteith method has been considered as a universal standard to estimate  $ET_0$  (Allen et al. 1989, 1994, 1998; Feddes and Lenselink 1994; Smith 1992; Sentelhas et al. 2010). There are several advantages to using the FAO Penman-Monteith method to estimate  $ET_0$ : (1) the method requires only one reference height, (2) it is less sensitive to omission of stability correction adjustments as compared to gradient methods, and (3) hourly, daily, and monthly  $ET_0$  can be calculated (Allen et al. 1994, 1998). Because of the stated advantages of the FAO Penman-Monteith method, it was used to calculate  $ET_0$  in this study.

Four kinds of weather data are required to estimate  $ET_0$  using the FAO Penman-Monteith method: temperature, solar radiation, wind, and relative humidity. Calculating  $ET_0$  using this method is not recommended if required data are missing. However, the FAO Penman-Monteith method provides alternative calculation procedures with missing data to estimate  $ET_0$  (Allen et al. 1998). The formulas of the FAO Penman-Monteith method used in this study were detailed in Appendix B.

## CHAPTER 3

### STUDY METHODS

The following sections explain what kinds of data were required in this study, how the required data were collected, and how the prediction models were developed using the data.

#### 3.1 Data collection

##### 3.1.1 Drying trials data

###### *3.1.1.1 Study sites description*

The four sites in this study were located near Corvallis, Butte Falls, Boardman, and Clatskanie (Figure 3.1). The Corvallis site ( $44^{\circ}41'49''\text{N}$ ,  $123^{\circ}20'22''\text{W}$ ) was located in central western Oregon and the Butte Falls site ( $42^{\circ}32'21''\text{N}$ ,  $122^{\circ}33'44''\text{W}$ ) was located in southwestern Oregon. They were in-forest study sites. The Boardman site ( $45^{\circ}46'39''\text{N}$ ,  $119^{\circ}32'22''\text{W}$ ) was located in north central Oregon and the Clatskanie site ( $46^{\circ}06'33''\text{N}$ ,  $123^{\circ}14'31''\text{W}$ ) was located in north western Oregon. They were off-forest study sites: a log storage yard near Clatskanie and an open space within a tree plantation near Boardman.

The sites were especially chosen to enable comparisons of the rate of changes in woody biomass moisture content under both wet and dry climate conditions: Corvallis and Clatskanie were considered to be the wetter sites and Butte Falls and Boardman were considered to be the drier sites.

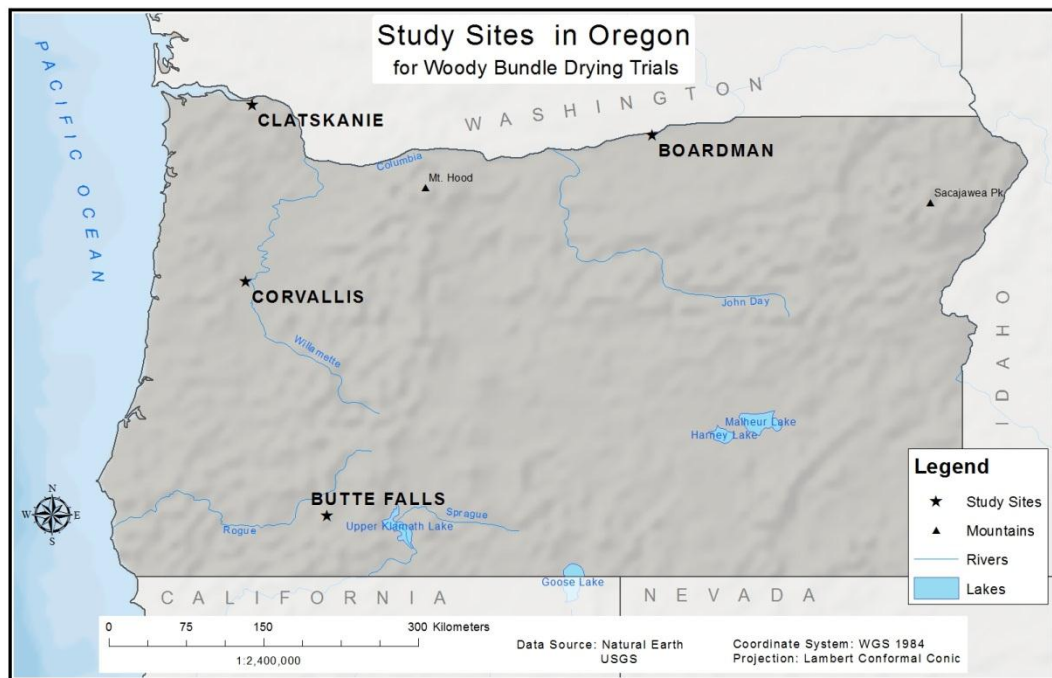


Figure 3.1 Map of study sites: representing locations of four study sites in Oregon which are Clatskanie, Boardman, Corvallis, and Butte Falls.

#### 3.1.1.2 Biomass bundles

To monitor changes of moisture contents in woody biomass, we built woody biomass bundles using freshly felled trees and let them dry in the air. Two different species were used in the drying trials depending on the study site; Douglas-fir was used in the Corvallis and Butte Falls study sites; hybrid poplar was used in the Boardman and Clatskanie study sites.

Douglas-fir was selected since it is a softwood and is one of the dominant species in forests of the Pacific Northwest (PNW). It is also the most common and commercially desirable timber species in the PNW. Hybrid poplar was selected since it is a hardwood and is of interest as a potential source of woody

biomass fuel because of its very high growth rates. Hybrid poplar can grow up to 2.4 meters per year and achieve heights of 20 to 30 meters in 6 to 12 years when managed using short-rotation silvicultural practices (Felix 2008). Hybrid poplar can produce between 8 and 22 metric tons of dry wood per hectare per year (ORNL date unknown). In comparison, Douglas-fir can produce between 1.4 and 2.3 metric tons of dry wood per hectare per year (Hermann and Lavender 1999).

At the Corvallis and Butte Falls study sites, woody biomass bundles were built using small Douglas-fir logs which were about 3 meter long and had an average diameter of about 156 mm. Drying trials were initiated four times at each study site between December 2010 and December 2011. At each trial, three bundles were built and each bundle was air dried under different canopy covers: open, intermediate, and closed. An area with open canopy was entirely free of canopy cover. An area with closed canopy had at least half of the surface area covered by canopy. Intermediate canopy was between the open and closed canopy condition. A total of 24 Douglas-fir biomass bundles were built over the study period and the average initial weight of the bundles was about 2,261 kg.

At the Clatskanie and Boardman study sites, woody biomass bundles were built using hybrid poplar trees. Two different drying trials were done at each study site between April 2011 and January 2012. At each trial, two different types of bundles were built: denoted as small and large. The small hybrid poplar bundles consisted of logs with average diameter of 82 mm. The average initial weight of the small bundles was about 3,444 kg. The large hybrid poplar bundles consisted logs with an average diameter of about 150 mm. Their average initial

weight was about 5,413 kg. A total of 8 hybrid poplar bundles were built over the study period; 4 small poplar bundles and 4 large poplar bundles. More detail on the bundle characteristics for both the Douglas-fir and hybrid poplar bundles is provided in Appendix A (Tables A. 1 to 4). Photos showing examples of the bundles are provided in Appendix A (Figures A. 2 to 3).

Bundles were weighed when first built, at the end of each trial, and at approximately 10 day intervals in-between. 200HS Battery Digital Hanging Scales, measuring to the nearest 1 kg, were used at the Corvallis, Butte Falls and Clatskanie sites. Bundles were lifted with a large hydraulic loader at each site. A Fairbanks truck scale, measuring to the nearest 9 kg, was used at the Boardman site.

In Europe it has been found that covering biomass can speed up drying rates by limiting input of new moisture from rainfall. Bundles at the Corvallis, Butte Falls and Clatskanie sites were partially covered with lumber wrapping paper to possibly speed up drying rates. Bundles at the Boardman site were also initially partially covered with lumber wrapping paper. However, strong winds at this site soon destroyed the covers and these were not replaced.

#### *3.1.1.3 Woody disks*

To determine initial and final moisture contents of the woody bundles, 30 woody disk samples (30 to 50 mm thick) were collected at the beginning and at the

end of each drying trial. At the beginning ten logs were randomly selected from a representative pile of logs and three disks per log were collected. Bundles were then built from the remaining logs in the pile. At the end of the trial ten logs were randomly selected from each bundle; three disks were collected from both sides and the center of each selected log due to possibly different drying rates in different portions of the logs. All woody disk samples were oven dried using the American Society for Testing and Materials (ASTM) standard D 2016 for four days at 103 degrees Celsius ( $\pm 2$  degrees). Initial moisture content means and standard errors, which were determined by the woody disks, for each bundle are provided in Appendix A (Tables A. 1 to 4).

### 3.1.2 Weather data

For developing the prediction models, the nearest weather stations to each study site were used to collect weather data over the period of the drying trials; specifically, precipitation, wind speed, minimum and maximum temperature, dewpoint temperature, and relative humidity were obtained. Weather data for the Corvallis study site were collected using a Davis Vantage VUE Pro weather station which was set up in December 2010. Weather data provided by the National Oceanic and Atmospheric Administration (NOAA) and by the Pacific Northwest Cooperative Agricultural Weather Network (AgriMet) were used for the other three study sites. The weather station for Corvallis site was located within 0.1 km from the location of the bundles. The weather data for the Butte Falls site were

provided by a weather station which was about 0.2 km to the northwest of the study site. The Boardman site used weather data from a weather station which was about 4.5 km to the north of the study site. Two sources of weather data were used for the Clatskanie site; data from a weather station about 9.9 km to the south of the study site was primarily used; some lost data were provided by a weather station which was about 12 km to the south of the site.

Oregon has been split into nine climate zones. Historic weather data provided by the AgriMet for the period between January 2010 and December 2011 was used to predict estimated air-drying times within four of the nine climate zones.

## **3.2 Modeling**

### **3.2.1 Data preparation**

The data needed to develop prediction models were first calculated in the data preparation stage. These were the moisture content of each bundle, the cumulative precipitation, and the cumulative  $ET_0$ .

Moisture contents (%) used in this thesis are expressed on a wet-basis, and are the ratio of moisture weight to the total weight of the woody biomass. The initial moisture content for each bundle was considered to be the average of the moisture contents for wood disks gathered at the beginning of each trial. When bundles were reweighed at approximately 10-day intervals, the assumption was made that any loss of weight was due to a loss of moisture and that the solid wood

content remained unchanged. Moisture contents were recalculated for each bundle for each monitoring date.

$ET_0$  (mm) was computed based on the daily collected weather data: precipitation (mm), mean wind speed ( $m\ s^{-1}$ ), relative humidity (%), minimum and maximum temperature ( $^{\circ}C$ ), and dewpoint temperature ( $^{\circ}C$ ). Precipitation data and  $ET_0$  data for each study site were individually summed to provide specific day cumulated precipitation and specific day cumulated  $ET_0$ . Bundles were not reweighed at exactly 10-day intervals. The different day intervals between measuring bundle weights was taken into consideration in determining the cumulated precipitation and  $ET_0$  data.

All moisture contents and  $ET_0$  were calculated in Microsoft Excel 2010. However, data preparations for predicting air-drying times at different locations in Oregon were done using Microsoft Visual Studio C++ 2010. Precipitation and calculated  $ET_0$  data were summed up in 10-day intervals for these predictions.

### 3.2.2 Drying models

Data normality tests, linear mixed-effects modeling and cross-validation were done to develop the drying prediction models. All statistical analyses were performed using the R statistical language, version 2.14.0 (<http://www.r-project.org>). To validate prediction models the cross-validation method was used; all prepared data for modeling were divided into two set of data: a developing data



set (85% of total data) and a validating data set (15% of total data). For developing the prediction models, moisture content, precipitation,  $ET_0$ , treatment data for canopy cover and diameter size, and specific interval days of monitoring (usually 10 days) in the developing data set were entered in R. In order to extend the use of the models spatially to other parts of Oregon and temporally to different seasons of the year, the prediction models were designed based on climate data.

Since the weights of each bundle were measured repeatedly at the same locations for the period of their drying trials, the data entered in R were fitted to linear mixed-effects models using the *nlme* package in R (Pinheiro and Bates 2000). Model selection was performed by the best subset procedure based on Akaike's information criterion (AIC) and on the significance of individual variables. The amount of moisture content change for the specific day period was predicted as a function of precipitation,  $ET_0$ , and treatment. The performance of the developed models was estimated using the validating data set by comparing actual moisture content and predicted moisture content.

Since the average monitoring interval of the drying trials was 10 days and this was considered to be a reasonable interval for checking the change of moisture in practice, the final drying models were developed to predict moisture content change for 10 day periods. Generally, freshly felled tree boles have moisture contents of 50 to 60% (Fraser 2002). In this study, the average initial moisture content of the bundles was 55%. However, a maximum moisture content of 30% is preferred for forest biomass use in small commercial boilers; moisture content which is too high can cause a boiler to shut down and boiler efficiency

dramatically drops when moisture contents are over 30% (Liang et al. 1996). Therefore, using the prediction models, drying times to reach moisture content of 30% from 55% were predicted for four different locations. The four locations were in different Oregon climate zones and were selected to demonstrate how drying times vary depending on different climatic conditions. The four locations were Bandon, OR (zone 1, coast), Corvallis, OR (zone 2, Willamette valley), Medford, OR (zone 3, southwestern valleys), and Bend, OR (zone 7, south central) (Appendix Figure A.1). The prediction models were also used to demonstrate the impact of four different harvesting seasons when drying began, namely the 1<sup>st</sup> day of January, April, July, and October. Predictions were based on historic weather data for a full two-year period.

## **CHAPTER 4**

### **RESULTS AND DISCUSSION**

#### **4.1 Actual drying times**

##### **4.1.1 Douglas-fir**

Air-drying curves for all of the Douglas-fir biomass bundles, which were monitored at Corvallis between 14 December 2010 and 12 December 2011, and at Butte Falls between 16 December 2010 and 8 December 2011 are shown on Figure 4.1. Standard errors for initial moisture were less than 2%. The drying curves for the two sites show similar drying patterns. There were changes in the moisture contents during spring and summer seasons (April to October). However, during fall and winter seasons (October to April), the moisture contents in the biomass bundles barely changed. In other words, spring and summer are moisture losing seasons for Douglas-fir biomass at Corvallis and Butte Falls. On the other hand, fall and winter are moisture stationary or gaining seasons. In addition, bundles drying under different canopy conditions had similar drying patterns.

Initial moisture contents for each drying trial were different (Tables A1 to A4). This may be due to a number of possible reasons. Depending on harvest schedules and logistics, logs may have been felled and left in the forest for up to several weeks before being used for bundle construction. Also, drying rates prior to bundling and the moisture content of the trees prior to felling may have varied with the season. Compared to the other drying trials, a different pattern of drying curves was found in the summer trial at Corvallis. However, the drying pattern is neither logical nor consistent.

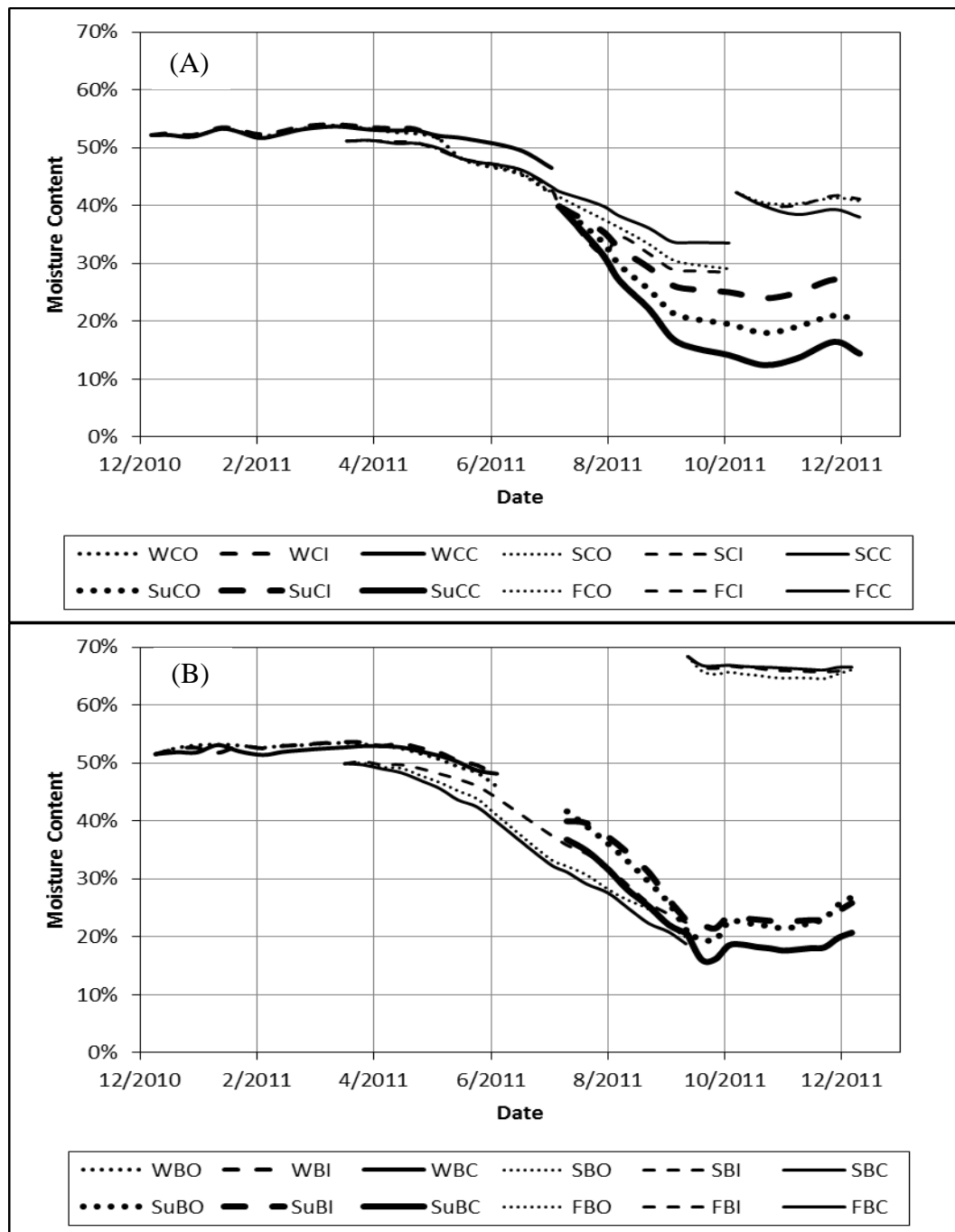


Figure 4.1 Drying curves of Douglas-fir biomass drying trials at Corvallis, OR (A) and at Butte Falls, OR (B). In the legends below each figure the first letter (or two) relates to the season in which drying began (W = Winter, S = Spring, Su = Summer, F = Fall), the middle letter relates to the study location (C = Corvallis, B = Butte Falls), the last letter relates to the canopy cover type (O = Open, I = Intermediate, C = Closed).

#### 4.1.2 Hybrid poplar

Air-drying trials using hybrid poplar biomass were carried out at Clatskanie between 12 May 2011 and 5 January 2012 and at Boardman between 12 April 2011 and 4 January 2012. Figure 4.2 shows the drying curves of both small and large hybrid poplar biomass bundles for the two study sites. The drying curves of the hybrid poplar biomass can be explained by two factors: 1) weather conditions and seasons, and 2) tree size. Depending on where and when the biomass bundles were air dried, the shapes of the drying curves are significantly different. The drying curves of both the Clatskanie and Boardman sites are decreasing, but at different rates, during the summer seasons (April to August). However, during winter seasons the shapes of the drying curves are different; only the curves of the Boardman site are decreasing. The rates of the drying curves are greater at the Boardman site than at the Clatskanie site for the entire study period. In addition, the rate of moisture content change depended on the log size within the bundles; the rates moisture content change for the small hybrid poplar biomass bundles are greater than the rates for the large hybrid poplar biomass bundles.

Poplar trees for small bundles were cut the same day that bundles were built. However, the trees for large bundles at Boardman were cut a week before the bundle were constructed. Thus, the initial moisture contents of large hybrid poplar bundles are relatively lower than the small hybrid poplar bundles at Boardman.

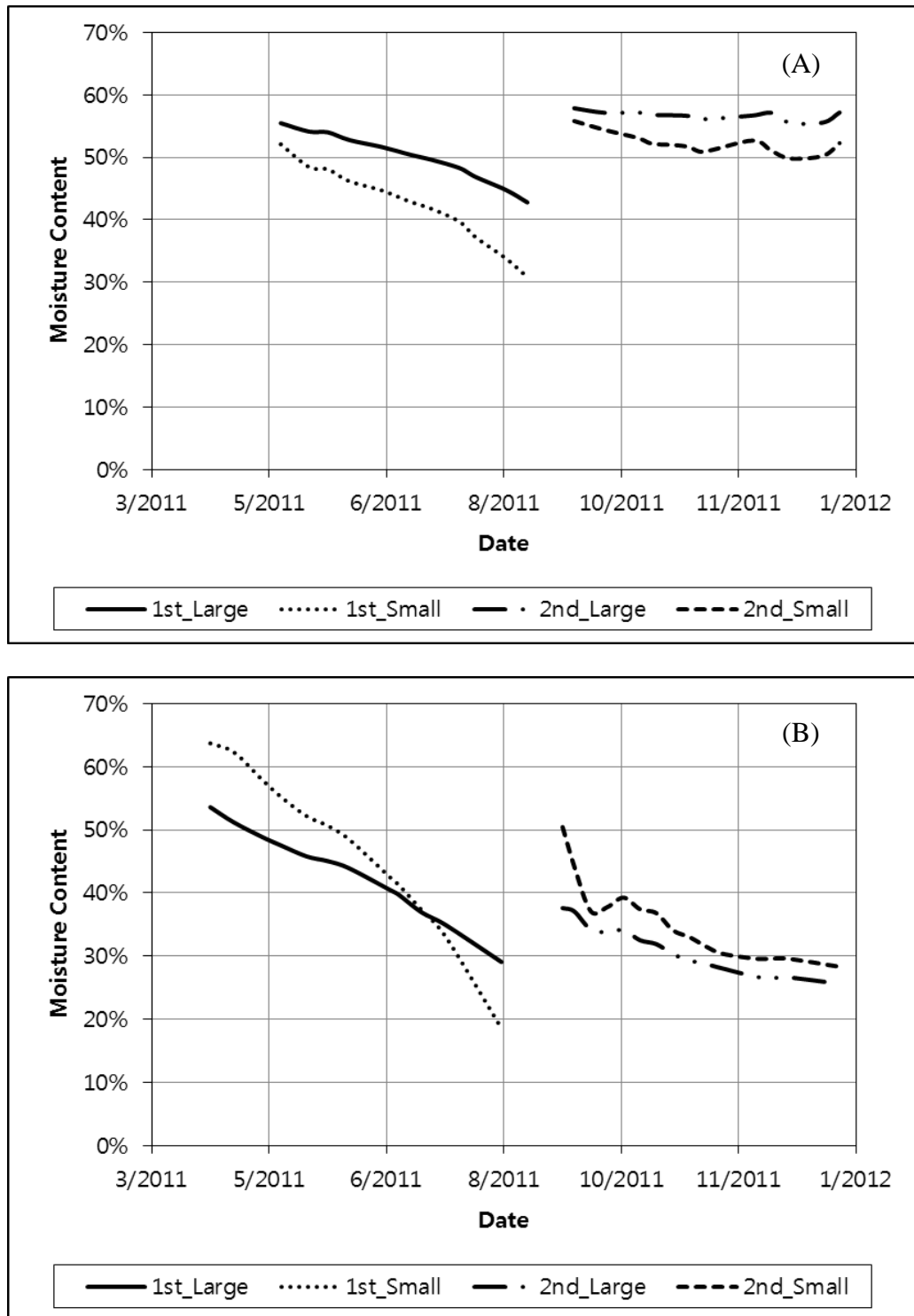


Figure 4.2 Drying curves of both small and large hybrid poplar biomass drying trials at Clatskanie (A) and at Boardman, OR (B). In the legends below each figure 1<sup>st</sup> = the first trial, 2<sup>nd</sup> = the second trial, Large = large biomass bundles and Small = small biomass bundles.

## 4.2 Prediction models

Many models were developed and evaluated before selecting the final set of prediction models. Prediction models were initially designed to predict final moisture content as a function of initial moisture content, cumulative precipitation, cumulative  $ET_0$ , number of days between measurements, and treatments of log size and canopy covers. However, the number of days and  $ET_0$  were highly correlated ( $-0.730$ ). In addition, the explanatory variables did not show significant relationships to the response variable (final moisture content). Log and reciprocal transformations were applied to both initial and final moisture content data to improve the performance of the model, however, no improvement was found. Therefore, the response variable was changed from final moisture content to the difference between the final moisture content and the initial moisture content over the number of days. The difference between final moisture content and initial moisture content over the number of days was then modeled as a function of initial moisture content, cumulative precipitation for the number of days, cumulative  $ET_0$  for the number of days, and treatments of log size and canopy covers. No significant relationships between the treatment of canopy cover and initial moisture content to the response variable were found, possibly due to the inconsistent and illogical pattern shown in the Corvallis drying curves. Therefore, the precipitation data,  $ET_0$ , and size treatment were considered as the best explanatory variables. Little correlation ( $< 0.162$ ) was found between the explanatory variables for both the Douglas-fir and hybrid poplar models.

Based on the collected moisture content data, weather data and the process stated above, two models were finally selected:

$$\Delta MC10 = -0.3932 - 0.03505 * ET10Day + 0.01363 * PP10Day \quad (1)$$

$$\Delta MC10 = -2.2774 - 0.01358 * ET10Day + 0.01566 * PP10Day + 1.1626 * SIZE \quad (2)$$

Where  $\Delta MC10^4$  is “moisture change” for a 10 day period (%); ET10Day, calculated cumulative  $ET_0^5$  for a 10 day period (mm); PP10Day, cumulative precipitation for a 10 day period (mm); SIZE, binary variable (0: Small Poplar, 1: Large Poplar).

Equation (1) is for Douglas-fir biomass and Equation (2) is for hybrid poplar. The models predict the amount of moisture content change at the end of a 10 day period as a function of ET10Day, PP10Day, and SIZE. Significant relationships were found between the response variable and the explanatory variables. There is a negative relationship between the change of moisture content and  $ET_0$ ; as  $ET_0$  increases, moisture content decreases. Precipitation and log size show positive relationships with the amount of moisture content change; as precipitation increases moisture content increases; bigger logs lose moisture slower than smaller logs. No specific relationship was found between the canopy cover treatment and the amount of moisture change in Douglas-fir.

---

<sup>4</sup>  $\Delta MC10$  is actual change of moisture (%) between initial moisture content (%) and final moisture content (%) for a 10 day period: final moisture content (%) equals initial moisture content (%) plus  $\Delta MC10$  (%).

<sup>5</sup>  $ET_0$  is not measured directly from weather stations, but is the reference ET calculated by using the FAO Penman-Monteith method.



### 4.3 Validation of prediction models

The developed prediction models for moisture content change were verified by comparing actual and predicted moisture contents on a validating data set (Figure 4.3). R-squared ( $R^2$ ) values between the models' prediction values and the actual values for Douglas-fir and hybrid poplar biomass were 0.99 and 0.97, respectively.

To understand how well the models fit to the actual drying curves, comparisons between actual and predicted drying curves were done. The best and worst fit bundle drying curves for each species were chosen to demonstrate their fitness (Figure 4.4 and Figure 4.5). The actual drying curves look smoother than the predicted drying curves in the worst fit figures. It would be difficult to find exact reasons for the differences; however, one probable reason was variability in time intervals between measurements (i.e., periods > 10 days).

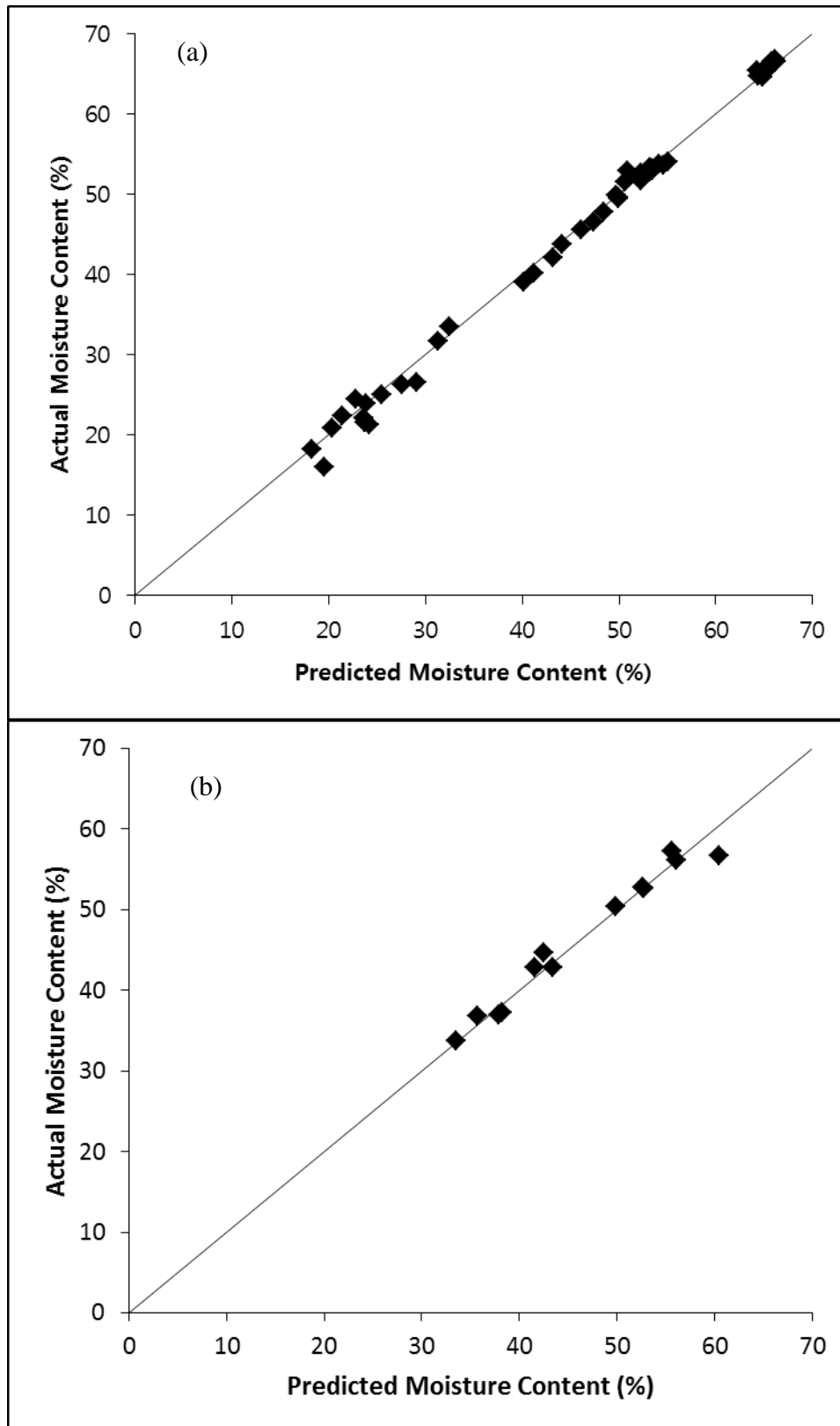


Figure 4.3 Relationships between actual and predicted moisture content for both Douglas-fir biomass (a) and hybrid poplar biomass (b)

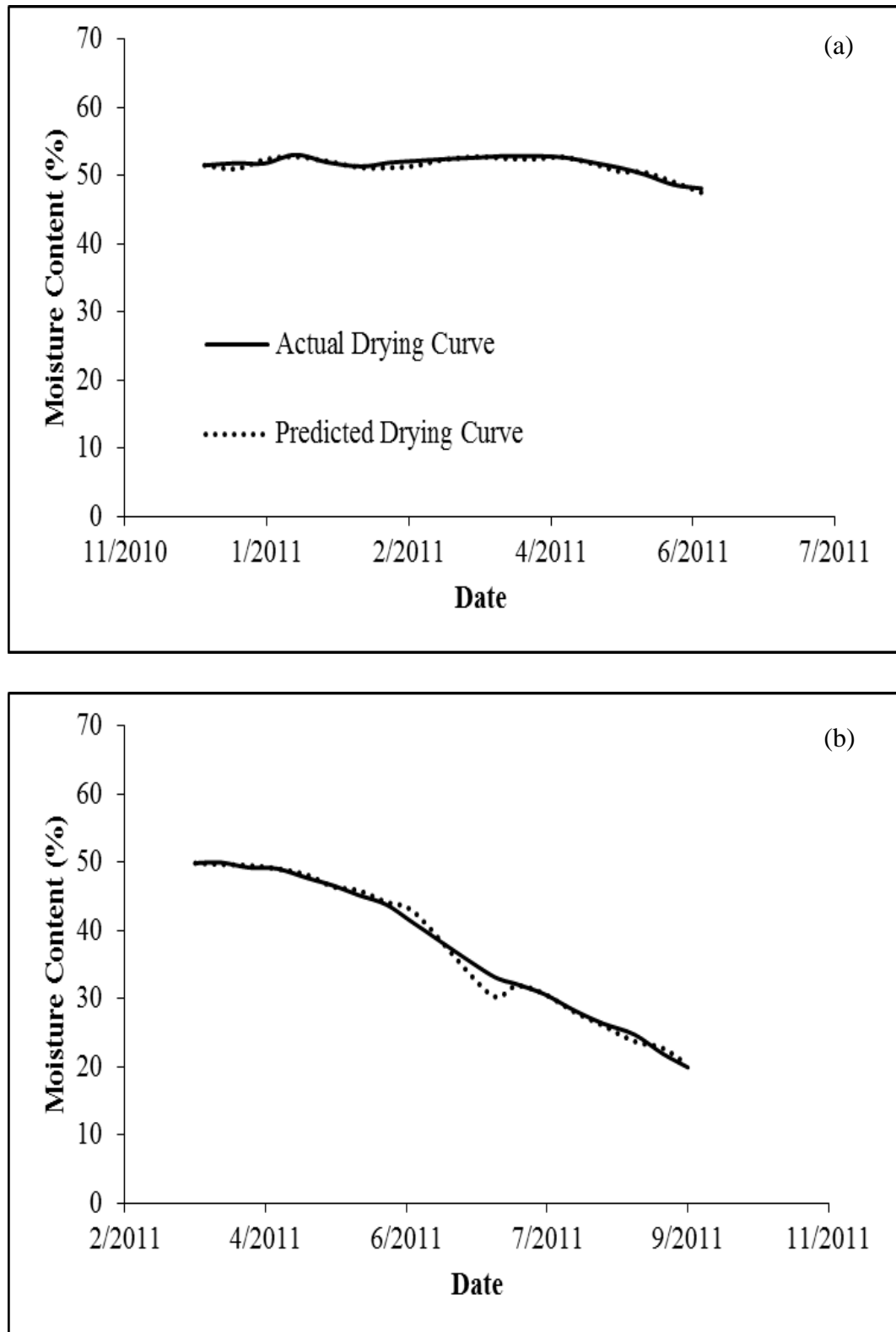


Figure 4.4 Actual and predicted drying curves for Douglas-fir biomass for two bundles chosen to represent the best (a) and worst (b) fits

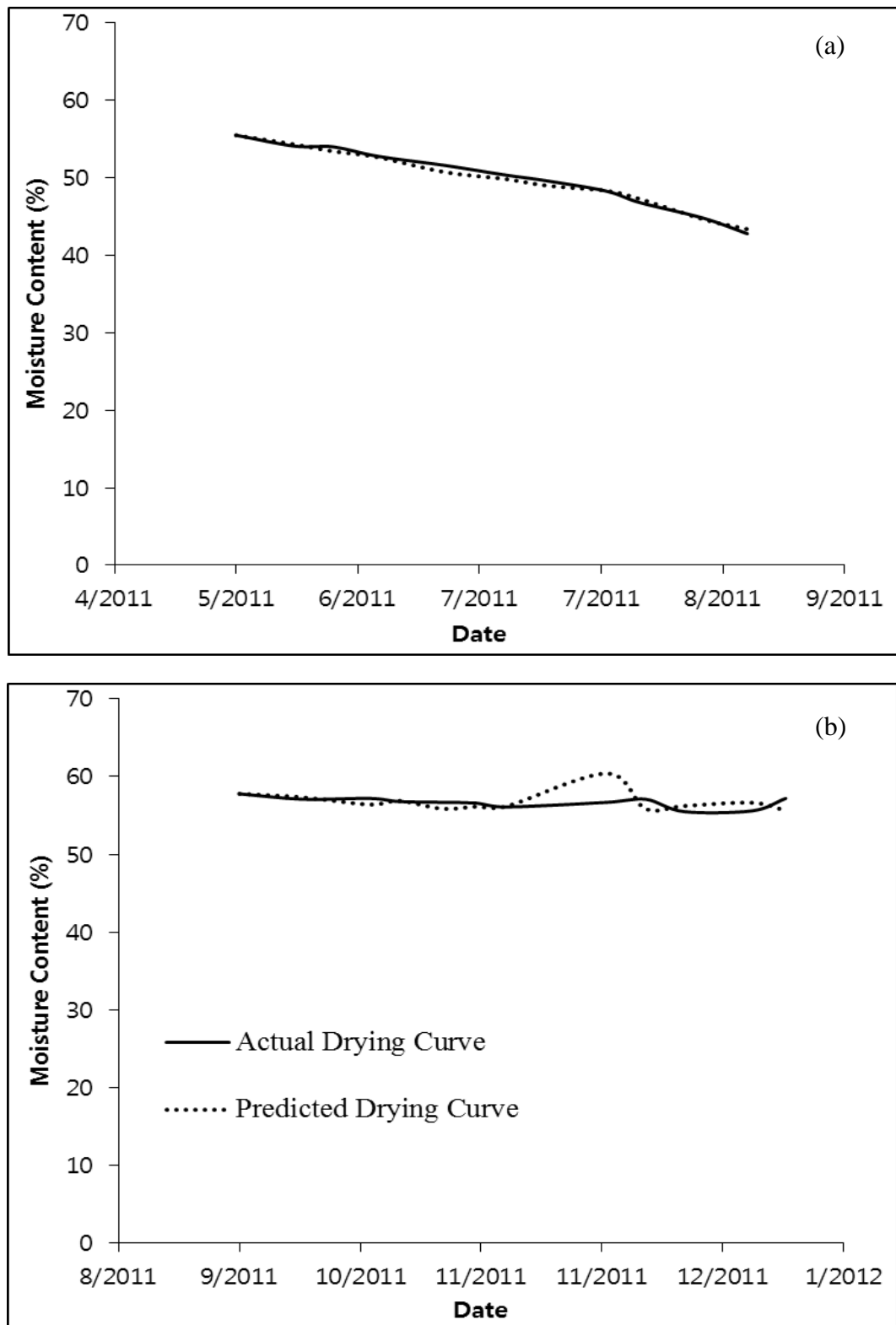


Figure 4.5 Actual and predicted drying curves for hybrid poplar biomass for two bundles chosen to represent the best (a) and worst (b) fits

#### 4.4 Predicted air-drying times

Air-drying times for both Douglas-fir and hybrid poplar biomass, at four locations in Oregon (representing four of Oregon's Climate Zones) and four different seasons, were predicted based on the developed models. The precipitation and evapotranspiration for these four locations were compared based on their weather data between 1 January 2010 and 31 December 2011 (Table 4.1). Among the four locations, the largest amount of cumulative precipitation (2,891 mm) was found in Bandon, OR (zone 1) and the smallest amount (462 mm) was found in Bend, OR (zone 7). Medford, OR (zone 3) had the largest amount of cumulative reference evapotranspiration (1,868 mm) and Bandon, OR (zone 1) had the smallest amount of cumulative reference evapotranspiration (1,179 mm).

Table 4.1 Total precipitation and reference evapotranspiration at four locations in Oregon for the period 1 January 2010 to 31 December 2011

Climate Zones	Precipitation (mm)	Reference Evapotranspiration * (mm)
Zone 1 (Bandon)	2,891	1,179
Zone 2 (Corvallis)	2,120	1,633
Zone 3 (Medford)	1,034	1,868
Zone 7 (Bend)	462	1,708

\* Calculated based on the FAO Penman-Monteith method

The number of days required to dry both Douglas-fir and hybrid poplar biomass from 55% moisture content to 30% moisture content was predicted for each location (Table 4.2, Table 4.3, and Table 4.4). The predicted days can be explained based on weather conditions caused by different seasons and locations.

#### 4.4.1 Prediction of air-drying days for Douglas-fir biomass

Table 4.2 Predicted number of days required to dry Douglas-fir biomass to 30% moisture content at four Oregon climate zones depending on different start months.

Start	Zone 1	Zone 2	Zone 3	Zone 7
Month	(Bandon)	(Corvallis)	(Medford)	(Bend)
Jan	595	248	209	207
April	490	175	144	151
July	439	352	259	252
Oct	>450	345	293	256

It took the largest number of days to reach 30% moisture when drying Douglas-fir biomass was started on 1<sup>st</sup> of January at Bandon (zone 1). Also, insufficient climate data was available to predict drying times based on the two full years when the drying was started on 1<sup>st</sup> of October at Bandon (zone 1), hence a value of >450 days. The smallest number of days were required at Medford (zone 3) when the drying was started on 1<sup>st</sup> of April. However, for most of the

year predictions indicated that fewer days would be required at Bend (zone 7) than at other locations. Compared to Medford (zone 3), it usually took more days at Corvallis (zone 2) to reach 30% moisture content for all the seasons (31 to 93 days more). At three of the four locations, except Bandon (zone 1), drying that was started in April could be expected to take the least number of days to reach 30% moisture content and drying that was started in October would be expected to take the largest number of days.

Based on the results in Table 4.2, it takes fewer days to dry Douglas-fir woody biomass in inland areas than in coastal areas in Oregon; the average difference in drying days between zone 1 and zone 7 was 277 days. Also, southern Oregon is better to dry Douglas-fir biomass to 30% moisture content than northern Oregon; the average difference in drying days between zone 2 and zone 3 was 54 days. Spring would be the best season and winter the worst season to start to dry Douglas-fir biomass.

#### 4.4.2 Prediction of air-drying days for hybrid poplar biomass

##### 4.4.2.1 *Small hybrid poplar*

Due to the small diameter size, the predicted drying days for small hybrid poplar biomass are much shorter than Douglas-fir and large hybrid poplar biomass. The range for the predicted time to dry for the four locations is 88 to 170 days. The largest number of predicted days to reach 30% moisture content was for Bandon (zone 1). The shortest number of days was for Medford (zone 3) when

the drying was started on 1<sup>st</sup> of July. However, when the whole year is taken into consideration Bend (zone 7) usually requires fewer days to reach the desired moisture content. Compared to northern Oregon, fewer days are required than woody biomass in southern Oregon; the average difference between predicted days for zone 2 and zone 3 was 14 days. Also, compared to coastal areas, inland areas are better for drying small hybrid poplar biomass; the average difference between predicted days for zone 1 (coast) and zone 7 (inland) was 44 days. Summer is the best season and winter is the worst season to start to dry small hybrid poplar biomass in Oregon.

Table 4.3 Predicted number of days required to dry small hybrid poplar biomass to 30% moisture content at four Oregon climate zones depending on different start months.

Start	Zone 1	Zone 2	Zone 3	Zone 7
Month	(Bandon)	(Corvallis)	(Medford)	(Bend)
Jan	168	132	115	106
April	123	106	99	96
July	101	92	88	91
Oct	170	148	122	92



#### 4.4.2.2 Large hybrid poplar

Due to its larger diameter size, large hybrid poplar took much longer to reach 30% moisture content than the small hybrid poplar biomass. The fewest number of days was taken at Bend (zone 7) when the drying was started on 1<sup>st</sup> of July. Bandon, Corvallis, Medford, then Bend ranked highest to lowest in the number of days to dry large hybrid poplar biomass to 30% moisture content. The largest number of days was taken when drying started on 1<sup>st</sup> of January at Bandon (zone 1). Comparing coastal (Bandon) and inland areas (Bend) in Oregon, it is better to dry large hybrid poplar biomass in inland areas; the average difference between predicted days for zone 1 and zone 7 was 44 days. Comparing northern Oregon (Corvallis) to southern Oregon (Medford), it takes fewer air-drying days in the south; the average difference between predicted days for zone 2 and zone 3 was 51 days. Spring is the best season and winter is the worst season to start to dry large hybrid poplar biomass in Oregon.

Table 4.4 Predicted number of days required to dry large hybrid poplar biomass to 30% moisture content at four Oregon climate zones depending on different start months.

Start	Zone 1	Zone 2	Zone 3	Zone 7
Month	(Bandon)	(Corvallis)	(Medford)	(Bend)
Jan	402	235	201	189
April	390	189	164	163
July	352	293	203	190
Oct	345	307	252	198

#### 4.4.2.3 Comparison of drying rates for large and small poplar

The ratio of the large poplar biomass log diameter to the small poplar biomass log diameter was 1.83. Based on this difference in size, the air-drying rate “rule of thumb” for lumber (Simpson et al. 1999) would indicate that the large poplar would take approximately 2.5 times as long to dry to the same moisture content as would the small poplar. Table 4.6 shows that the ratio of drying rates spanned 2.5 and varied between 1.7 and 3.5.

Table 4.5 Ratio of predicted number of days required to dry large hybrid poplar biomass, compared with small hybrid poplar biomass, to 30% moisture content at four Oregon climate zones depending on different start months.

Start	Zone 1	Zone 2	Zone 3	Zone 7
Month	(Bandon)	(Corvallis)	(Medford)	(Bend)
Jan	2.4	1.8	1.8	1.8
April	3.2	1.8	1.7	1.7
July	3.5	3.2	2.3	2.1
Oct	2.0	2.1	2.1	2.2

## **CHAPTER 5**

### **CONCLUSIONS**

#### **5.1 General conclusions and limitations**

This study was performed: (1) to measure changes in moisture content for Douglas-fir and hybrid poplar harvested at different locations in Oregon and at different times of the year, (2) to develop a model which can be used to predict estimated biomass air-drying times for these species at any time of the year and at any location where historic weather data are available and (3) to demonstrate use of the models for predicting the variation in drying times between different climate zones in Oregon.

Air-drying rates vary logically with the dominant climatic patterns of the area, such that southern Oregon sites and spring/summer months tend to dry the fastest. Prediction models for rate of drying are strong using weather data and reference  $ET_0$ , as well as material size when it is available. Since these models are based on climate data, the use of the models can be extended spatially to other parts of Oregon and temporally to different seasons of the year. This conclusion is in agreement with that of Liang et al. (1996) who found, for another species (bundled *Leucaena*) and another region (Hawaii) that climate data could be used to predict drying rates for biomass harvested in different seasons and at different locations.

This study, however, was limited to developing prediction models for only two species and for bundled, woody biomass material in small log form with the

bark largely present. Generally, different tree species have different densities which can result in different drying rates; higher density species tend to have lower drying rates than lower density species (Houck and Eagle 2007; Simpson 1999).

The size of bundles was not specifically evaluated in this study; however, it seems that the size of materials (diameter of logs) within the bundle is a more critical factor for drying rate than the size of bundles judged by the actual drying curves of this study. The models should be used with caution to estimate air-drying times for woody biomass bundles that contain logs that are considerably different in size to those within this study (156 mm average diameter for Douglas-fir trees and 82 mm or 150 mm average diameter for hybrid poplar). As noted by Simpson et al. (1999) and found in this study drying times for woody material increase non-linearly as a function of thickness.

The drying rates found in this study were considerably lower than those reported by Simpson and Wang (2003) for small Douglas-fir logs. However, the small logs used in their study were debarked and then stacked with gaps between the logs to facilitate air-flow; both these practices are known to speed up drying rates.

Future research should be focused on improving the performance of prediction models by extending the models to more tree species and to a wider range of biomass materials and sizes, including biomass residues. Both diameter and length of logs or limbs should be considered as parameters for the size of biomass materials. The effects of bundle size, or biomass pile size for loosely

stacked material, should be specifically investigated since these were not included in this study. In addition, the developed models should be validated in other climate regions, so that more generalized models could eventually be developed.

## **5.2 Management implications**

Understanding how moisture content changes with changing locations, seasons, and operational practices is very important for improving the utilization of woody biomass as an energy source. Moisture management, through storage and drying in the supply chain between harvesting and utilization, is key to improving both transportation costs and market values.

Storing material in the forest to allow drying is likely to lead to lower transportation costs. However, there are also likely to be added costs associated with managing the stored material; for example, knowing where it is, when it was harvested, and when it is due to be uplifted.

Since drying rates are dependent on species and season in which harvesting was undertaken, there may be difficulties associated with obtaining an even flow throughout the year of energy material with a consistent moisture content. For example, material harvested in October and dried to 30% moisture content may be ready for in-forest processing and transport to the customer at the same time as material harvested in April of the following year. In addition, stands with mixed species could end up with material either dried to different moisture

contents or require multiple visits to the same area to process and transport the material.

Since drying rates will also depend on material size, there are likely to be different storage periods required for material coming from final harvests versus thinnings and from longer rotation lengths.

The optimal storage method, location and drying time are economic decisions and can be evaluated using wood fuel calculation models such as those developed by Kofman and Murphy (2010) for the Wood Energy program in Ireland. An essential prerequisite for selecting the optimal drying method and time, however, is the ability to predict the number of days required to reach a specified moisture content. Thus, the air-drying rate models developed from this study, along with future improvements, could be usefully utilized in many fields related to the forest biomass for energy business. These models may be of benefit to the management of hybrid poplar tree farms, biomass hauling companies, biomass harvesting companies, and biomass plants, among other businesses.

## BIBLIOGRAPHY

- Allen, R.G., Jensen, M.E., Wright, J.L., and R.D. Burman. 1989. Operational estimate of reference evapotranspiration. *Agronomy Journal*. 81: 650-662
- Allen, R.G., Pereira, L.S. Raes, D. and M. Smith. 1998. Crop evapotranspiration: Guidelines for computing crop water requirements. *Irrigation and Drainage*. Paper 56. UN-FAO, Rome, Italy.
- Allen, R.G., Smith, M., Perrier, A. and L.S. Pereira. 1994. An update for the definition of reference evapotranspiration. *ICID Bulletin* 43(2): 1-34.
- American Society for Testing and Materials. 1988. D 2016-74 (Reapproved 1983): Standard Test Methods for Moisture Content of Wood. 1988 Annual Book of ASTM Standards. Section 4. Vol. 04.09. West Conshohocken, Pennsylvania.
- Bergman, R. and J. Zerbe. 2004. Primer on Wood Biomass for Energy. Madison, Wisconsin, USDA Forest Service:  
[http://www.fpl.fs.fed.us/documnts/tmu/biomass\\_energy/primer\\_on\\_wood\\_biomass\\_for\\_energy.pdf](http://www.fpl.fs.fed.us/documnts/tmu/biomass_energy/primer_on_wood_biomass_for_energy.pdf) (accessed 4/27/2012)
- Biomass Research and Development Technical Advisory Committee & Biomass Research and Development Initiative. (2007, October). Roadmap for bioenergy and biobased products in the United States.:  
[http://www1.eere.energy.gov/biomass/pdfs/obp\\_roadmapv2\\_web.pdf](http://www1.eere.energy.gov/biomass/pdfs/obp_roadmapv2_web.pdf) (accessed 4/27/2012)
- Energy Information Administration. 2010. International Energy Outlook; Energy Information Administration: Washington, D.C.:  
<http://www.eia.gov/oiaf/archive/aeo10/index.html> (accessed 4/27/2012)

- Feddes, R.A. and K.J., Lenselink. 1994. Evapotranspiration. In: Drainage Principles and Applications. ILRI Publication, 16:145-173, Wageningen.
- Felix, E., Tilley, D.R., Felton, G. and E. Flamino. 2008. Biomass production of hybrid poplar (*Populus* sp.) grown on deep-trenched municipal biosolids. *Ecological Engineering*. 33: 8–14.
- Fraser, I. A. 2002. Making Forest Policy Work. Kluwer Academic Publishers. The Netherlands.
- Hermann, K., R. and D. P. Lavender. 1999. Douglas-fir planted forests. *New Forests* 17(1-3): 53-70.
- Houck, J.E. and B. N. Eagle. 2007. Hardwood or softwood? *Hearth & Home*. January: 49-50.
- Jirjis, R. 1995. Storage and drying of wood fuel. *Biomass and Bioenergy* 9(1-5): 181-190.
- Johansson, J., Liss, J-E., Gullberg, T. and R. Bjorheden. 2006. Transport and handling of forest energy bundles – advantages and problems. *Biomass and Bioenergy*. 30(4): 334-341.
- Kofman, P.D. and T. Kent. 2007. Harvesting and processing forest biomass for energy production in Ireland. The ForestEnergy 2006 programme. COFORD, Dublin.
- Kofman, P.D. and G.E. Murphy 2010. Wood fuel cost calculator. Available from Wood Energy Ireland on <http://www.woodenergy.ie/documentspublications/software/> (accessed 06/19/2012).



Labędzki, L., Kanecka-Geszke, E., Bak, B. and S. Slowinska. 2011. Estimation of reference evapotranspiration using the FAO Penman-Monteith method for climatic conditions of Poland.:

<http://www.intechopen.com/books/evapotranspiration/estimation-of-reference-evapotranspiration-using-the-fao-penman-monteith-method-for-climatic-conditi> (accessed 4/27/2012)

Liang, T., Khan, M.A., and Q. Meng. 1996. Spatial and temporal effects in drying biomass for energy. *Biomass and Bioenergy* 10(5-6): 353-360.

McDonald, T., Rummer, B., Taylor, S. and J. Valenzuela. 2001. Potential for shared log transport services. P. 115-120. In *Proceedings of the 24th Annual Council on Forest Engineering Meeting*. Snowshoe Mountain, West Virginia. Wang, J. et al. (eds.). Council on Forest Engineering, Corvallis, OR.

McDonald, T., Stokes, B. and J. McNeel. 1995. Effect of product form, compaction, vibration and comminution on energywood bulk density. In: *Proceedings of a Workshop on Preparation and Supply of High Quality Wood Fuels; 1994 June 13-16; Garpenberg, Sweden: IEA/BA Task IX; 6-23.*

ORNL (date unknown) Popular Poplars: Trees for many purposes, Biomass Feedstock Development Program Fact Sheet, Oak Ridge National Laboratory. <http://bioenergy.ornl.gov/misc/poplars.html>. (accessed 4/27/2012)

Pan, F., Han, H.-S., Johnson, L. and W. Elliot. 2008. Production and cost of harvesting and transporting small-diameter trees for energy. *Forest Products Journal* 58(5): 47-53.

- Payne, S., Dutzik, T. and E. Figdor. 2009. The high cost of fossil fuels: why America can't afford to depend on dirty energy?:  
<http://cdn.publicinterestnetwork.org/assets/c54f63c712cd336e233821bf5cb28aff/US-The-High-Cost-of-Fossil-Fuels-text--cover.pdf> (accessed 4/27/2012)
- Perlack R.D., Wright, L.L., Turhollow, A.F., Graham, R.L., Stokes, B.J. and D.C. Erbach. 2005. Biomass as feedstock for a bioenergy and bioproducts industry: The technical feasibility of a billion-ton annual supply. Joint study sponsored by the US Department of Energy and US Department of Agriculture. ORNL/TM-2005/66. Oak Ridge, TN: Oak Ridge National Laboratory.
- Pettersson, M., and T. Nordfjell. 2007. Fuel quality changes during seasonal storage of compacted logging residues and young trees. *Biomass and Bioenergy* 31(11-12): 782-792.
- Pinheiro, J. C. and D. M. Bates. 2000. *Mixed-Effects Models in S and S-PLUS*. Springer. New York.
- Ranta, T. and S. Rinne. 2006. The profitability of transporting uncomminuted raw materials in Finland. *Biomass and Bioenergy* 30(3):231-237.
- Robert D. 2007. *Woody Biomass - A renewable energy source: a fact sheet from the West Forestry Consortium*. USDA For. Serv. Res. Note MT-31.
- Ronnqvist, M., Sahlin, H. and D. Carlsson. 1998. Operative planning and dispatching of forestry transportation. Linkoping Institute of Technology, Sweden. Report LiTH-MAT-R-1998-18. 31pp.
- Rummer, B. 2008. Assessing the cost of fuel reduction treatments: a critical review. *Forest Policy and Economics* 10(6):355-362.

- Sentelhas P.C., Gillespie T.J. and E.A. Santos. 2010. Evaluation of FAO Penman-Monteith and alternative methods for estimating reference evapotranspiration with missing data in Southern Ontario, Canada. *Agricultural Water Management* 97: 635–644.
- Simpson, W. T., Tschernitz, J. L. and J. J. Fuller. 1999. Air drying of lumber. Gen. Tech. Rept. FPL-GTR-117. USDA Forest Serv., Forest Prod. Lab., Madison, WI. 62 p.
- Simpson, W.T. and X. Wang. 2003. Estimating air drying times of small-diameter ponderosa pine and Douglas-fir logs. Res. Pap. FPL.RP.613. Madison, WI: U.S. Department of Agriculture, Forest Service, Forest Products Laboratory. 14 p. Department of Agriculture, Forest Service, Forest Products
- Smith, M. 1992. Report on the expert consultation on revision of FAO methodologies for crop water requirements. Land and Water Development Division, FAO, Rome.
- Stokes, B.J., Watson, W.F., and D.E. Miller. 1987. Transpirational drying of energywood. ASAE Paper 87-1350. St. Joseph, MI: American Society of Agricultural Engineers, 14 p.
- Thornthwaite, C.W. 1948. An approach towards a rational classification of climate. *Geographical Review* 38(1): 55-94.
- Trenberth, K. E. 1998. Atmospheric moisture residence times and cycling: Implications for rainfall rates with climate change. *Climatic Change*, 39, 667–694.

## APPENDIX A

Figures and tables relating to the drying trials

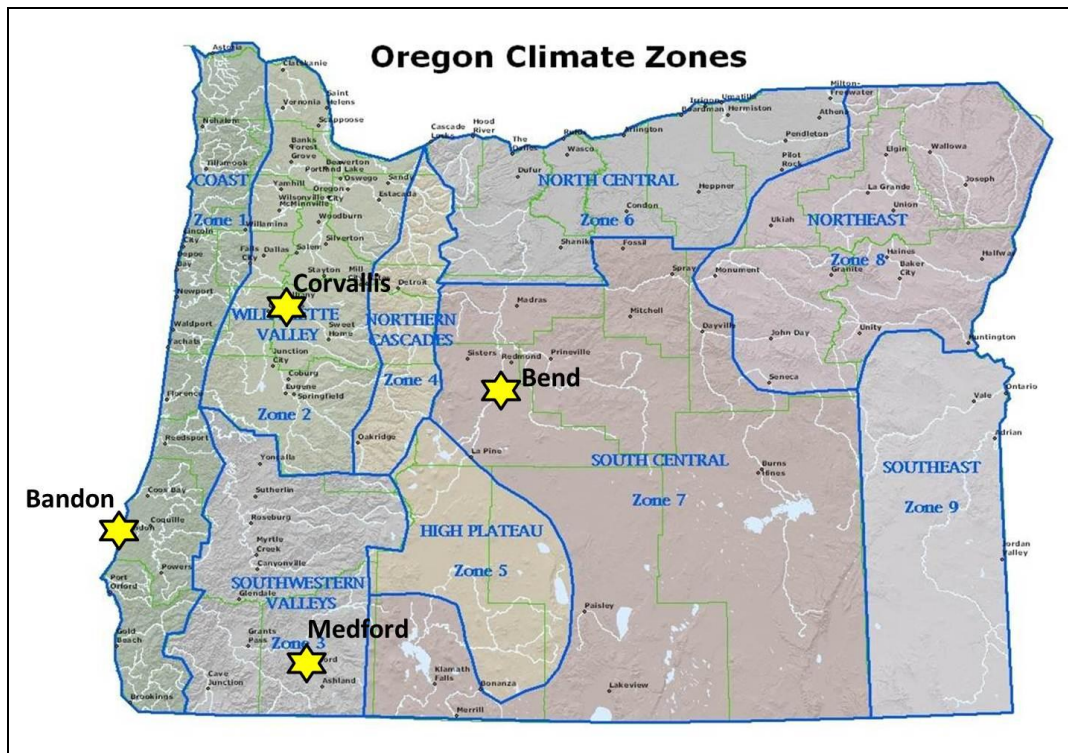


Figure A.1 The map of Oregon Climate Zones with the general locations of sites used for predicting air-drying times.

([http://oregon.gov/ODA/NRD/weather.shtml#Weather\\_forecasts](http://oregon.gov/ODA/NRD/weather.shtml#Weather_forecasts))

Table A.1 Information relating to Douglas-fir bundles at Corvallis

Bundle	Average	Initial	Initial Moisture Content (%)	
	Diameter (mm)	Weight (kg)	Mean	Standard Error
Winter_Open	178	3,211	52	1.9
Winter_Intermediate	178	3,060	52	1.9
Winter_Closed	163	3,093	52	1.9
Spring_Open	175	2,673	51	1.0
Spring_Intermediate	172	1,914	51	1.0
Spring_Closed	181	3,139	51	1.0
Summer_Open	173	1,500	40	1.9
Summer_Intermediate	155	1,812	40	1.9
Summer_Closed	145	2,166	40	1.9
Fall_Open	176	1,689	42	1.1
Fall_Intermediate	173	1,712	42	1.1
Fall_Closed	184	1,856	42	1.1

Table A.2 Information relating to Douglas-fir bundles at Butte Falls

Bundle	Average Diameter (mm)	Initial Weight (kg)	Initial Moisture Content (%)	
			Mean	Standard Error
Winter_Open	169	2,744	52	1.1
Winter_Intermediate	154	3,621	52	1.1
Winter_Closed	150	2,900	52	1.1
Spring_Open	152	2,827	50	0.9
Spring_Intermediate	150	3,143	50	0.9
Spring_Closed	145	2,117	50	0.9
Summer_Open	114	1,316	42	Not available
Summer_Intermediate	143	1,588	40	1.5
Summer_Closed	132	1,397	37	Not available
Fall_Open	114	1,538	68	1.0
Fall_Intermediate	143	1,481	68	1.0
Fall_Closed	132	1,767	68	1.0

Table A.3 Information relating to hybrid poplar bundles at Clatskanie

Bundle	Average	Initial	Initial Moisture Content (%)	
	Diameter (mm)	Weight (kg)	Mean	Standard Error
1st_Large	131	4,245	55	0.3
1st_Small	80	3,271	52	0.7
2nd_Large	131	3,901	58	0.8
2nd_Small	82	2,849	56	1.0

Table A.4 Information relating to hybrid poplar bundles at Boardman

Bundle	Average	Initial	Initial Moisture Content (%)	
	Diameter (mm)	Weight (kg)	Mean	Standard Error
1st_Large	139	7,013	54	0.4
1st_Small	101	5,389	64	0.6
2nd_Large	199	6,495	38	1.0
2nd_Small	66	2,268	50	0.1





Figure A.2 Douglas-fir bundle construction using a large hydraulic loader (above) and air-drying Douglas-fir bundles under the intermediate canopy cover (bottom)





Figure A.3 Cross section of the large hybrid poplar bundle (above) and weighing a small hybrid poplar bundle using a crane scale and large hydraulic loader (bottom)

## APPENDIX B

### Formulas to calculate the reference evapotranspiration

The following formulas were used in this study to calculate the reference  $ET_0$ .

All formulas were adopted by Allen et al. (1998) and more detail can be found in Allen et al. (1998).

(Equation 1)  $ET_0$ : reference evapotranspiration [ $\text{mm day}^{-1}$ ]

$$ET_0 = \frac{0.408\Delta(R_n - G) + \gamma \frac{900}{T + 273} u_2 (e_s - e_a)}{\Delta + \gamma (1 + 0.34u_2)}$$

where

$ET_0$ : reference evapotranspiration [ $\text{mm day}^{-1}$ ]

$R_n$ : net radiation at the crop surface [ $\text{MJ m}^{-2} \text{day}^{-1}$ ] from (Equation 20)

$G$ : soil heat flux density, 0 [ $\text{MJ m}^{-2} \text{day}^{-1}$ ] (which can be ignored due to its small magnitude)

$T$ : air temperature at 2 m height [ $^{\circ}\text{C}$ ] from (Equation 4)

$u_2$ : wind speed at 2 m height [ $\text{m s}^{-1}$ ] from collected weather data

$e_s$ : saturation vapor pressure [ $\text{kPa}$ ] from (Equation 6)

$e_a$ : actual vapor pressure [ $\text{kPa}$ ] from (Equation 8)

$e_s - e_a$ : saturation vapor pressure deficit [ $\text{kPa}$ ] from (Equation 9)

$\Delta$ : slope vapor pressure curve [ $\text{kPa } ^{\circ}\text{C}^{-1}$ ] from (Equation 7)

$\gamma$ : psychrometric constant [ $\text{kPa } ^{\circ}\text{C}^{-1}$ ] from (Equation 3)

(Equation 2)  $P$ : atmospheric pressure [ $\text{kPa}$ ]

$$P = 101.3 \left( \frac{293 - 0.0065z}{293} \right)^{5.26}$$

where

$P$ : atmospheric pressure [ $\text{kPa}$ ]

$z$ : station elevation above sea level [ $\text{m}$ ]

(Equation 3)  $\gamma$ : psychrometric constant [kPa °C<sup>-1</sup>]

$$\gamma = \frac{c_p P}{\varepsilon \lambda} = 0.665 \times 10^{-3} P$$

where

$\gamma$ : psychrometric constant [kPa °C<sup>-1</sup>]

P: atmospheric pressure [kPa] from (Equation 2)

$\lambda$ : latent heat of vaporization, 2.45 [MJ kg<sup>-1</sup>]

$c_p$ : specific heat at constant pressure, 1.013 10<sup>-3</sup> [MJ kg<sup>-1</sup> °C<sup>-1</sup>]

$\varepsilon$ : ratio molecular weight of water vapor/dry air = 0.622

(Equation 4)  $T_{\text{mean}}$ : the mean daily air temperature (°C)

$$T_{\text{mean}} = \frac{T_{\text{max}} - T_{\text{min}}}{2}$$

Where

$T_{\text{mean}}$ : the mean daily air temperature (°C)

$T_{\text{max}}$ : the daily maximum air temperature (°C)

$T_{\text{min}}$ : the daily minimum air temperature (°C)

(Equation 5)  $e^\circ(T_{\text{max}})$ : the maximum saturation vapor pressure [kPa] and

$e^\circ(T_{\text{min}})$ : the minimum saturation vapor pressure [kPa]

$$e^\circ(T) = 0.6108 \exp \left[ \frac{17.27T}{T + 237.3} \right]$$

T will be  $T_{\text{max}}$  and  $T_{\text{min}}$  for  $e^\circ(T_{\text{max}})$  and  $e^\circ(T_{\text{min}})$ , respectively.

(Equation 6)  $e_s$ : the mean saturation vapor pressure [kPa]

$$e_s = \frac{e^\circ(T_{\text{max}}) + e^\circ(T_{\text{min}})}{2}$$

Where  $e^\circ(T_{\text{max}})$  and  $e^\circ(T_{\text{min}})$  are given by (Equation 5).

(Equation 7)  $\Delta$ : slope vapor pressure curve [kPa °C<sup>-1</sup>]

$$\Delta = \frac{4098 \left[ 0.6108 \exp \left( \frac{17.27 T}{T + 237.3} \right) \right]}{(T + 237.3)^2}$$

where

$\Delta$ : slope vapor pressure curve [kPa °C<sup>-1</sup>]

T: mean air temperature [°C] from (Equation 4)

(Equation 8)  $e_a$ : actual vapor pressure [kPa]

$$e_a = e^o(T_{\text{dew}}) = 0.6108 \exp \left[ \frac{17.27 T_{\text{dew}}}{T_{\text{dew}} + 237.3} \right]$$

where

$e_a$ : actual vapor pressure [kPa]

$T_{\text{dew}}$ : dewpoint temperature [°C]

(Equation 9)  $e_s - e_a$ : saturation vapor pressure deficit [kPa]

$e_s$  and  $e_a$  are given by (Equation 6) and (Equation 8), respectively.

(Equation 10)  $R_a$ : extraterrestrial radiation [MJ m<sup>-2</sup> day<sup>-1</sup>]

$$R_a = \frac{24(60)}{\pi} G_{sc} d_r [\omega_s \sin(\varphi) \sin(\delta) + \cos(\varphi) \cos(\delta) \sin(\omega_s)]$$

where

$R_a$ : extraterrestrial radiation [MJ m<sup>-2</sup> day<sup>-1</sup>]

$G_{sc}$ : solar constant = 0.0820 [MJ m<sup>-2</sup> day<sup>-1</sup>]

$d_r$ : inverse relative distance Earth-Sun [rad] from (Equation 12)

$\omega_s$ : sunset hour angle [rad] from (Equation 14)

$\varphi$ : latitude [rad] from (Equation 11)

$\delta$ : solar declination [rad] from (Equation 13)

(Equation 11)  $\phi$ : latitude [rad]

$$[\text{Radians}] = \frac{\pi}{180} [\text{decimaldegrees}]$$

(Equation 12)  $d_r$ : inverse relative distance Earth-Sun [rad]

$$d_r = 1 + 0.033 \cos\left(\frac{2\pi}{365} J\right)$$

Where

J: the number of the day in the year

(Equation 13)  $\delta$ : solar declination [rad]

$$\delta = 0.409 \sin\left(\frac{2\pi}{365} J - 1.39\right)$$

Where

J: the number of the day in the year

(Equation 14)  $\omega_s$ : sunset hour angle [rad]

$$\omega_s = \arccos [-\tan(\phi) \tan(\delta)]$$

Where  $\phi$  and  $\delta$  are given by (Equation 11) and (Equation 13), respectively.

(Equation 15) N: Daylight hours

$$N = \frac{24}{\pi} \omega_s$$

Where  $\omega_s$  is the sunset hour angle in radians given by (Equation 14).

(Equation 16)  $R_s$ : solar or shortwave radiation [ $\text{MJ m}^{-2} \text{ day}^{-1}$ ]

$$R_s = k_{Rs} \sqrt{(T_{\max} - T_{\min})} R_a$$

where

$R_a$ : extraterrestrial radiation [ $\text{MJ m}^{-2} \text{ d}^{-1}$ ] from (Equation 10)

$T_{\max}$ : maximum air temperature [ $^{\circ}\text{C}$ ]

$T_{\min}$ : minimum air temperature [ $^{\circ}\text{C}$ ]

$k_{Rs}$ : adjustment coefficient for interior region (0.16) and costal region(0.19)  
[ $^{\circ}\text{C}^{-0.5}$ ]

(Equation 17)  $R_{so}$ : clear-sky radiation [ $\text{MJ m}^{-2} \text{ day}^{-1}$ ]

$$R_{so} = (0.75 + 2 \cdot 10^{-5} \cdot z) R_a$$

Where  $z$  is station elevation above sea level [m] and  $R_a$  is extraterrestrial radiation [ $\text{MJ m}^{-2} \text{ d}^{-1}$ ] given by (Equation 10).

(Equation 18)  $R_{ns}$ : net solar or shortwave radiation [ $\text{MJ m}^{-2} \text{ day}^{-1}$ ]

$$R_{ns} = (1 - \alpha) R_s$$

where

$R_{ns}$ : net solar or shortwave radiation [ $\text{MJ m}^{-2} \text{ day}^{-1}$ ]

$\alpha$ : albedo or canopy reflection coefficient, which is 0.23 for the hypothetical grass reference crop [dimensionless]

$R_s$ : extraterrestrial radiation [ $\text{MJ m}^{-2} \text{ d}^{-1}$ ] given by (Equation 16)

(Equation 19)  $R_{nl}$ : net outgoing longwave radiation [ $\text{MJ m}^{-2} \text{ day}^{-1}$ ]

$$R_{nl} = \sigma \left[ \frac{T_{\max, K}^4 + T_{\min, K}^4}{2} \right] \left( 0.34 - 0.14 \sqrt{e_a} \right) \left( 1.35 \frac{R_s}{R_{so}} - 0.35 \right)$$

where

$R_{nl}$ : net outgoing longwave radiation [ $\text{MJ m}^{-2} \text{ day}^{-1}$ ]

$\sigma$ : Stefan-Boltzmann constant [ $4.903 \times 10^{-9} \text{ MJ K}^{-4} \text{ m}^{-2} \text{ day}^{-1}$ ]

$T_{\max, K}$ : maximum absolute temperature during the 24-hour period

[ $K = ^\circ\text{C} + 273.16$ ]

$T_{\min, K}$ : minimum absolute temperature during the 24-hour period [ $K = ^\circ\text{C} + 273.16$ ]

$e_a$ : actual vapor pressure [kPa]

$R_s/R_{so}$ : relative shortwave radiation (limited to  $\leq 1.0$ )

$R_s$ : solar radiation [ $\text{MJ m}^{-2} \text{ day}^{-1}$ ] from (Equation 16)

$R_{so}$ : clear-sky radiation [ $\text{MJ m}^{-2} \text{ day}^{-1}$ ] from (Equation 17)

(Equation 20) Net radiation ( $R_n$ )

$$R_n = R_{ns} - R_{nl}$$

Where

$R_n$ : the net radiation [ $\text{MJ m}^{-2} \text{ day}^{-1}$ ]

$R_{ns}$ : net solar or shortwave radiation [ $\text{MJ m}^{-2} \text{ day}^{-1}$ ] from (Equation 18)

$R_{nl}$ : net outgoing longwave radiation [ $\text{MJ m}^{-2} \text{ day}^{-1}$ ] from (Equation 19)